

Exotic surface behaviors induced by geometrical settings of the two-dimensional dimerized quantum XXZ model

WenJing Zhu,¹ Chengxiang Ding,^{2,*} Long Zhang,^{3,†} and Wenan Guo^{1,4,‡}

¹*Department of Physics, Beijing Normal University, Beijing 100875, China*

²*School of Science and Engineering of Mathematics and Physics,
Anhui University of Technology, Maanshan, Anhui 243002, China*

³*Kavli Institute for Theoretical Sciences and CASD Center for Excellence in Topological Quantum Computation,
University of Chinese Academy of Sciences, Beijing 100190, China*

⁴*Beijing Computational Science Research Center, Beijing 100193, China*

(Dated: January 28, 2022)

We study the surface behavior of the two-dimensional columnar dimerized quantum antiferromagnetic XXZ model with easy-plane anisotropy, with particular emphasis on the surface critical behaviors of the (2+1)-dimensional quantum critical points of the model that belong to the classical three-dimensional O(2) universality class, for both $S = 1/2$ and $S = 1$ spins using quantum Monte Carlo simulations. We find completely different surface behaviors on two different surfaces of geometrical settings: the dangling-ladder surface, which is exposed by cutting a row of weak bonds, and the dangling-chain surface, which is formed by cutting a row of strong bonds along the direction perpendicular to the strong bonds of a periodic system. Similar to the Heisenberg limit, we find an ordinary transition on the dangling-ladder surface for both $S = 1$ and $S = 1/2$ spin systems. However, the dangling-chain surface shows much richer surface behaviors than in the Heisenberg limit. For the $S = 1/2$ easy-plane model, at the bulk critical point, we provide evidence supporting an extraordinary surface transition with a long-range order established by effective long-range interactions due to bulk critical fluctuations. The possibility that the state is an extraordinary-log state seems unlikely. For the $S = 1$ system, we find surface behaviors similar to that of the three-dimensional classical XY model with sufficiently enhanced surface coupling, suggesting an extraordinary-log state at the bulk critical point.

I. INTRODUCTION

At bulk critical points, surface states may emerge with novel critical phenomena beyond the bulk critical properties [1–5]. Typically, there are three classes of such surface states, namely, ordinary, special, and extraordinary, e.g., the three surface states of the classical O(n) model in dimension $d > 3$ at its bulk critical point. The fixed point of the extraordinary state corresponds to the bulk transition occurring in the presence of an ordered surface. This can happen if surface couplings are strong enough, such that the surface orders before the bulk when the temperature is lowered. On the other hand, if the surface couplings are the same in the bulk, one expects an ordinary transition, where singularities of the state come entirely from the bulk criticality. The special point is a multicritical point separating the ordinary and extraordinary states. This picture is supported by renormalization group theory [3, 4].

However, due to the Mermin-Wagner theorem [6], it is widely accepted that there is no extraordinary state, thus, there is no special state, for the $n \geq 2$ O(n) model in dimension $d = 3$, since the two-dimensional (2D) surface of the model cannot hold long-range order. Recently, Metlitski proposed a field-theoretical study to investigate

the classical O(n) model with n being continuously varied and suggested a new extraordinary-log class of the surface states for $n = 2$ and $n = 3$, where the surface correlation function decays as a power of $\log(r)$ [7]. Some predictions in this work have been verified in classical three-dimensional (3D) O(3) and classical 3D O(2) models. [8, 9]

For unfrustrated quantum systems, the d -dimensional SU(2) quantum critical point can be described by the $(d+1)$ -dimensional classical O(3) universality class, according to the quantum to classical mapping. Therefore, similar surface critical behaviors (SCBs) are expected for $d = 2$ quantum critical points in the 3D O(3) universality class. However, some unexpected behaviors were found for the surface transitions of the quantum critical points.

For dimerized antiferromagnetic Heisenberg systems, where the couplings are not distributed homogeneously on the lattice and are directionally anisotropic, thus making it possible to expose different surfaces by geometrical settings, one finds different SCBs on different surfaces without adapting surface couplings. [10–12] In particular, on the surface formed by dangling spins, nonordinary SCBs are found. The mechanism of such behavior is not yet clear. It was attributed to the surface capturing the gapless state in the bulk gapped phase due to topological θ -term of the $S = 1/2$ antiferromagnetic dangling spin chain. However, later research on the $S = 1$ dimerized Heisenberg antiferromagnet showed similar nonordinary SCBs on the dangling-spin surface, in which the topological- θ term is absent and the surface

* dingcx@ahut.edu.cn

† longzhang@ucas.ac.cn

‡ wguo@bnu.edu.cn

is thus gapped in the bulk disordered phase[13]. This has led to the above scenario being doubted.

The symmetry-protected topological (SPT) state[14, 15] offers another possible mechanism for such nonordinary SCBs of quantum criticality in the 3D O(3) universality class [10, 16]. In a recent paper[16], we showed that the surface perpendicular to the coupled topological $S = 1$ Haldane chains displays nonordinary SCBs, which is understood as the ends of the chains forming an $S = 1/2$ chain, which is gapless through the bulk gapped phase and thus forces the system to enter a nonordinary surface critical state.

To date, for the SCBs of the 3D O(2) universality class, only classical models have been studied [5, 9]. The SCBs of the quantum criticality belonging to the 3D O(2) universality class, especially with the quantum nature of spins, i.e., $S = 1/2$ and $S = 1$ involved, have not been investigated. In consideration of the new and interesting phenomena that have been observed and the mechanisms that are under debate in quantum models of the 3D O(3) universality class, it would be beneficial to study quantum models hosting the quantum criticality in the 3D O(2) universality class. In this work, we study the surface critical behaviors of 2D columnar dimerized (CD) spin- S quantum antiferromagnetic (QAF) XXZ models with easy-plane anisotropy that host quantum phase transitions from the Néel state to the quantum dimer state, which belongs to the classical 3D O(2) universality class, using unbiased quantum Monte Carlo simulations. Similar to the dimerized antiferromagnetic Heisenberg model studied previously, which is the isotropic limit of the current model, we form and study dangling-ladder and dangling-chain surfaces.

The dangling-ladder surface (to be specified in Sec. II) is gapped in the bulk gapped phase for both $S = 1/2$ and $S = 1$. Without tuning the surface couplings, it is natural to expect ordinary SCBs on this surface. Indeed, we observe ordinary SCBs in the dangling-ladder surface for both $S = 1/2$ and $S = 1$ spins.

However, we observe different surface behaviors in the dangling-chain surface (to be specified in Sec. II) for the $S = 1/2$ and $S = 1$ models.

On this surface, the $S = 1$ model behaves similarly to the classical 3D O(2) model with large surface couplings, where we find a transition in the bulk gapped phase, which can be understood as a Berenzinsky-Kosterlitz-Thouless (BKT) transition [17–19]. Further, the surface SCBs seem to belong to the extraordinary-log fixed point [7] at the bulk critical point.

For the $S = 1/2$ model, we find unexpected behaviors, e.g., divergence of the scale surface correlation length ξ_1/L preceding the bulk critical point, and crossings of ξ_1/L for different system sizes in the bulk gapped phase, considering that the surface is already critical as a Tomonaga-Luttinger liquid (TLL) [20, 21] in the dimerized limit. One scenario to understand this is that there is a new surface state, between the transition point and the bulk critical point, with spin-spin correlation decay-

ing as a power of $\log(r)$, different from the TLL, and with a finite correlation length to the bulk. We do not have a clear understanding of this phase and the corresponding phase transition. However, a transition from two different two phases without long-range order is not excluded by the Mermin-Wagner theorem [6]. Such transitions have been found in 2D O(2) [22] and 2D O(3) [23] systems. Furthermore, as found in classical models, a changing in the interaction range, not necessarily infinite, can drive the phase to another fixed point[24]. However, although the data can be fit according to the proposed scaling formula, the fits are not stable upon gradually excluding small systems. It is more likely that the correlation behaves finally cross over to normal TLL behavior. In the end, it is more plausible that the divergence of ξ_1/L are results of bulk critical behavior.

At the bulk critical point, we further study the SCBs of the dangling-chain edge. Our numerical results support an extraordinary SCB with long-range order established by effective long-range interactions due to bulk critical correlations. The possibility that the surface shows extraordinary-log behaviors seems unlikely.

This paper is organized as follows. Sec. II describes the models and methods. The observables used to investigate the surface states are also defined. In Sec. III, we present the results of the SCBs on the dangling-ladder surface. Sec. IV describes the studies of the SCBs on the dangling chain surfaces. In Sec. V, we conclude the paper.

II. MODELS AND METHOD

We study the columnar dimerized spin- S quantum antiferromagnetic XXZ model on the 2D square lattice, as shown in Fig. 1. The Hamiltonian of the model is given by

$$H = J \sum_{\langle i,j \rangle} D_{ij} + J' \sum_{\langle i,j \rangle'} D_{ij}, \quad (1)$$

where J and J' represent weak and strong antiferromagnetic couplings, denoted by black and blue bonds, respectively; $D_{ij} = S_i^x S_j^x + S_i^y S_j^y + \Delta S_i^z S_j^z$, with Δ the anisotropy parameter. We set $J = 1$ and let $g = J'/J > 1$ be the tuning parameter driving phase transition.

By tuning the anisotropy parameter Δ away from 1, the system breaks the SU(2) symmetry down to the U(1) symmetry in easy-plane with $\Delta \in [0, 1)$ or Z_2 symmetry in easy-axis z with $\Delta > 1$. The system undergoes a conventional Wilson-Fisher transition from the Néel state breaking the U(1) symmetry to the dimerized state in the 3D O(2) universality class by tuning g in the easy-plane case or a transition from the Néel state breaking the Z_2 symmetry to the dimerized state in the 3D Ising universality class in the easy-axis case. Here, we focus on the $S = 1/2$ and $S = 1$ easy-plane models.

In this work, we adopt the stochastic series expansion (SSE) [25] quantum Monte Carlo (QMC) method with loop algorithms [26, 27] to simulate the above models.

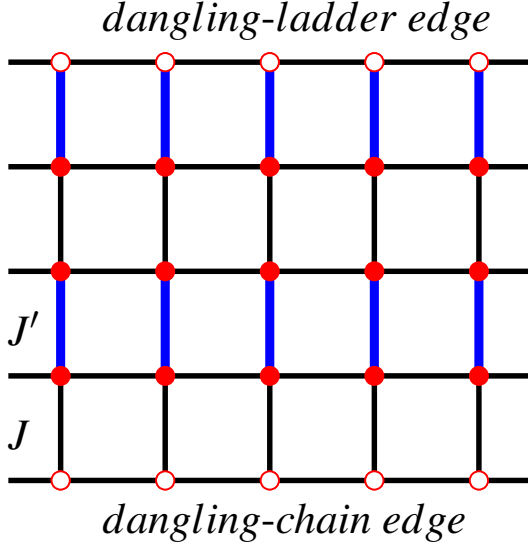


FIG. 1. Columnar dimerized easy-plane QAF XXZ model with open boundaries indicated by open red circles. $J(J')$ are antiferromagnetic XXZ couplings denoted by black (blue) bonds. By maintaining periodic boundary conditions in the x direction, the model exposes a dangling-chain edge (below) and a dangling-ladder edge (upper) by cutting J' and J bonds, respectively.

We have specified $L_x = L_y = L$, where L_x and L_y are linear lattice sizes along x and y direction, respectively. The inverse temperature β scales as $2L$ to calculate the bulk critical points and as L to study the SCBs of the models, respectively, considering the dynamical critical exponent $z = 1$ for the bulk criticality. Typically, 10^7 Monte Carlo samples are taken to calculate the average and estimate each data point's errorbar.

The bulk critical properties for a given Δ and S are obtained by finite-size scaling analyses on the spin stiffness obtained by quantum Monte Carlo simulations. The results are listed in Table I. More details are presented in Appendix A.

TABLE I. Bulk quantum critical points (QCPs) and exponents ν for the columnar dimerized easy-plane QAF XXZ models of given Δ and S . We also list properties published in the literature for the reader's convenience.

| Type | S | Δ | g_c | ν |
|------|-----|----------|-----------------|----------|
| CD | 1/2 | 0.5 | 2.73227(5) | 0.67(1) |
| | 1/2 | 0.9 | 2.1035(1) | 0.672(4) |
| | 1 | 0.9 | 6.01(1) | 0.66(1) |
| | 1/2 | 1 | 1.90951(1) [28] | |
| | 1 | 1 | 5.2854(6) [13] | |

To investigate the SCBs, we apply periodic boundary conditions in the x direction and expose open boundaries

by cutting J or J' bonds along the x direction. The open boundaries are indicated by open red circles in Fig. 1. Note that the boundary exposed by cutting J bonds exhibits a gapped ladder in the limit $g \rightarrow \infty$. Hence, this boundary is referred to as the dangling-ladder surface. The edge exposed by cutting a row of J' bonds is referred to as the dangling-chain edge, as it behaves as a quantum chain in the large g limit.

We adopt the squared surface staggered magnetization m_{s1}^2 and the surface spin-spin correlations to characterize the surface critical behaviors. These quantities depend on two equal-time spin-spin correlations defined as

$$C^{XY}(i, j) = \langle (S_i^x S_j^x + S_i^y S_j^y) \rangle \quad (2)$$

and

$$C^Z(i, j) = \langle S_i^z S_j^z \rangle. \quad (3)$$

While $C^Z(i, j)$ can be directly estimated in the S^z representation, the in-plane correlation $C^{XY}(i, j)$ is calculated through the following Green function

$$G(i, j) = \frac{1}{2} (\langle S_i^+ S_j^- \rangle + \langle S_i^- S_j^+ \rangle), \quad (4)$$

which is determined efficiently with an improved estimator by using the loop updating algorithm in the SSE QMC simulations.[29, 30]

The surface parallel correlation $C_{\parallel}(L/2)$ averages $C^{XY}(i, j)$ between two surface spins i and j at the longest distance $L/2$ over the surface under consideration, and the perpendicular correlation function $C_{\perp}(L/2)$ averages $C^{XY}(i, j)$ between two spins i and j at the longest distance $L/2$, where i is fixed on the surface and j is located at the center of the bulk, with the direction from i to j perpendicular to the surface.

The squared surface staggered magnetization is defined as

$$m_{s1}^2 = \frac{1}{L^2} \langle (\sum_{i \in \text{surface}} (-1)^i S_i^x)^2 + (\sum_{i \in \text{surface}} (-1)^i S_i^y)^2 \rangle, \quad (5)$$

where i labels the spins on the surface, which can be expressed with the Green function defined in Eq. (4),

$$m_{s1}^2 = \frac{2}{L^2} \sum_{i, j \in \text{surface}} (-1)^{i+j} G(i, j) \quad (6)$$

where i, j are the spins on the surface.

In addition, we calculate the surface second-moment correlation length

$$\xi_1 = \frac{L}{2\pi} \sqrt{\frac{S_1(q)}{S_1(q + \Delta q)} - 1}, \quad (7)$$

with $q = \pi$ and $\Delta q = 2\pi/L$, where the surface spin structure factor $S_1(q)$ is the Fourier transform of the surface spin-spin correlation $C_{\parallel}^{XY}(r_{ij})$ which averages $C^{XY}(i, j)$ between two surface spins i and j at the distance $r_{ij} = |j - i|$

$$S_1(q) = \frac{1}{\sqrt{L}} \sum_{i, j \in \text{surface}} e^{-iq(j-i)} C_{\parallel}^{XY}(r_{ij}). \quad (8)$$

III. SURFACE CRITICAL BEHAVIORS OF THE DANGLING-LADDER EDGE

In this section, we study the dangling-ladder edge of the $S = 1/2$ and $S = 1$ models. This edge is formed by “nondangling” spins, see Fig. 1 (the top edge). It is also called nondangling surface.

For the $S = 1/2$ quantum spin models with $SU(2)$ symmetry, the bulk transition is in the classical 3D $O(3)$ universality class. [31] For the dangling-ladder edge, the surface critical exponents are found in agreement with the ordinary universality class [11, 12]. This surface state is understandable since the edge can be viewed as a dangling ladder in the gapped dimer phase, and the ladder is gapped since it has two legs, thus effectively forming an integer-spin chain. It is different from the edge formed by dangling spins, as shown in Fig. 1 (the bottom edge), which is gapless in the gapped dimer phase, as a result, the surface critical behavior is nonordinary [11, 12]. When the symmetry of the model is down to $U(1)$, the gapped nature of the dangling ladder does not change. Therefore, we expect ordinary SCBs of 3D $O(2)$ class on the edge. Our numerical results, as shown below, confirm this.

For the $S = 1$ critical system in the 3D $O(3)$ universality class, the dangling-ladder edge is gapped as well. It was found that the SCBs are the ordinary transition of the 3D $O(3)$ universality class [13]. When the symmetry is down to $U(1)$, ordinary SCBs of the 3D $O(2)$ universality class are expected and verified by our numerical results discussed in this section.

We simulated $S = 1/2$ systems with linear sizes up to $L = 256$ and $S = 1$ systems with linear size up to $L = 96$. The quantities $\xi_1/L, C_{\parallel}(L/2), C_{\perp}(L/2)$ and $m_{s1}^2 L$ were calculated.

In Fig. 2 (a), we show the scaled surface correlation length ξ_1/L as a function of the system size L on a log-log scale. It is clear that the quantity converges to zero algebraically. By fitting data to the following formula [10],

$$\xi_1/L \propto L^{-p}, \quad (9)$$

we find $p = 0.681(5)$ for the $\Delta = 0.5$ $S = 1/2$ model, $p = 0.69(1)$ for the $\Delta = 0.9$ $S = 1/2$ model, and $p = 0.67(2)$ for the $\Delta = 0.9$ $S = 1$ model. The decay of ξ_1/L to zero shows that the surface correlation length diverges more slowly than the bulk correlation length ξ . Further, the surface critical behavior is controlled by ξ .

Figure 2 (b) shows the parallel correlation $C_{\parallel}(L/2)$ and perpendicular correlation $C_{\perp}(L/2)$ as functions of the system size L on a log-log scale. Both decay as power laws. We expect the following finite-size scaling behavior for them [10–12]:

$$C_{\parallel}(L/2) = L^{-(d+z-2+\eta_{\parallel})}(a + bL^{-\omega}), \quad (10)$$

and

$$C_{\perp}(L/2) = L^{-(d+z-2+\eta_{\perp})}(a + bL^{-\omega}), \quad (11)$$

where η_{\parallel} and η_{\perp} are two surface anomalous dimensions, $\omega > 0$ represents the effective exponent controlling corrections to scaling, which differs in the above two equations; $d + z$ is the space-time dimension with $d = 2$ and $z = 1$ in the current models.

The squared surface staggered magnetization $m_{s1}^2(L)$ obeys the following finite-size scaling form [10, 11] for $d = 2$ and $z = 1$:

$$m_{s1}^2 L = c + L^{2y_{h1}-3}(a + bL^{-\omega}), \quad (12)$$

in which y_{h1} is the scaling dimension of the surface staggered magnetic field h_1 ; c is a nonuniversal constant representing analytic correction to scaling due to surface. As shown in Fig. 2(c), $m_{s1}^2 L$ converges to a constant c as $L \rightarrow \infty$ for all three cases studied.

By gradually excluding small system sizes, we obtain statistically sound fits of Eq. (10), Eq. (11) and Eq. (12) without corrections to scaling for the $S = 1/2$, $\Delta = 0.5$ and 0.9 systems, and for the $S = 1$ and $\Delta = 0.9$ systems, respectively.

For the $S = 1/2$ spins, in the case $\Delta = 0.5$, we find $\eta_{\parallel} = 1.34(2)$, $\eta_{\perp} = 0.644(6)$, and $y_{h1} = 0.82(1)$; for $\Delta = 0.9$, we obtain $\eta_{\parallel} = 1.41(2)$ and $\eta_{\perp} = 0.69(2)$, and $y_{h1} = 0.80(1)$. The exponents for the two different Δ are consistent within 2 error bars. For the $S = 1$ case, we find exponents $\eta_{\parallel} = 1.51(1)$, $\eta_{\perp} = 0.65(1)$, and $y_{h1} = 0.74(5)$ for $\Delta = 0.9$. These results are listed also in Table II.

The exponents y_{h1} estimated for these models are close to those found for the ordinary SCB in the classical 3D $O(2)$ models [5, 32, 33].

The surface critical exponents are expected to satisfy the following scaling relations [2, 34, 35]

$$2\eta_{\perp} = \eta_{\parallel} + \eta \quad (13)$$

and

$$\eta_{\parallel} = d + z - 2y_{h1} \quad (14)$$

with η being the anomalous magnetic scaling dimension of the bulk transition in the $d + z$ spacetime. For the easy-plane XXZ model with $U(1)$ symmetry in two dimensions, we have $d + z = 3$ and $\eta = 0.038$ [36]. The exponents found for SCBs of the easy plane XXZ models with variant Δ and S satisfy or nearly satisfy the above scaling relations within error bars. The relatively large deviation for the $S = 1$ $\Delta = 0.9$ model might be because the simulated system sizes are not large enough.

TABLE II. SCB exponents for the dangling-ladder edge of the CD easy-plane XXZ models. The exponents y_{h1} of the three models are close to $y_{h1} = 0.781(2)$ found for the ordinary surface transition of the classical 3D $O(2)$ model [5].

| Type | S | Δ | η_{\parallel} | η_{\perp} | y_{h1} |
|------|-----|----------|--------------------|----------------|----------|
| CD | 1/2 | 0.5 | 1.34(2) | 0.644(6) | 0.82(1) |
| | 1/2 | 0.9 | 1.41(2) | 0.69(2) | 0.80(3) |
| | 1 | 0.9 | 1.51(1) | 0.65(1) | 0.74(5) |

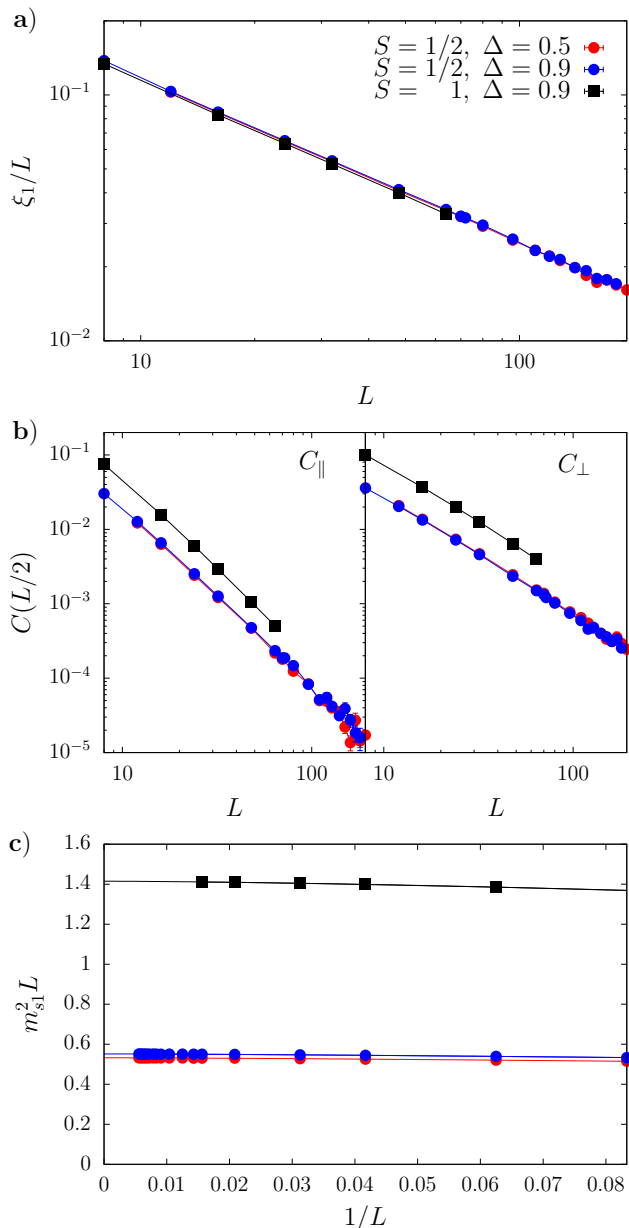


FIG. 2. Surface quantities on the dangling-ladder edge for the CD easy-plane XXZ model at the bulk QCPs with $\Delta = 0.5$ and 0.9 for the $S = 1/2$ case and $\Delta = 0.9$ for the $S = 1$ case. a) The scaled surface correlation length ξ_1/L as a function of L on a log-log scale. b) The surface parallel correlation function $C_{||}(L/2)$ and the perpendicular correlation function $C_{\perp}(L/2)$ as a function of L on a log-log scale. c) The scaled surface magnetization $m_{s1}^2 L$ vs $1/L$.

IV. SURFACE CRITICAL BEHAVIORS OF DANGLING-CHAIN EDGE

We now consider the dangling-chain edge for the CD QAF easy-plane XXZ model with $0 \leq \Delta \leq 1$.

For the $SU(2)$ CD models, the dangling-chain edge undergoes nonordinary SCBs with exponents close to the

special transition of the 3D $O(3)$ universality class [11, 12]. This was attributed to the fact that the edge is gapless due to the topological θ term of the $S = 1/2$ dangling chain in the gapped bulk state; when approaching g_c , the edge and bulk become gapless simultaneously, leading to the nonordinary surface transition [10, 11]. However, this scenario was challenged by the finding of Weber and Wesel that the same dangling-chain edge of the $S = 1$ model shows similar nonordinary SCBs. [13]

In a recent work on an improved classical 3D $O(3)$ model [8], Parisen Toldin found that the surface exponent y_s is relatively small and argued that the small value of y_s leads to a large region of surface coupling, where effectively the scaling of SCBs is governed by the special fixed point, and the observed exponents are thus close to the special SCBs and this offers an understanding of the nonordinary SCBs of the $S = 1$ quantum Heisenberg model. For the $S = 1/2$ quantum Heisenberg model, Jian and coauthors argued that if the special transition occurs in the presence of VBS order, $\eta_{||}$ should equal to the $S = 1$ value, due to a direct magnetic-VBS transition [37]. The nonperturbative effect due to the topological θ term to $\eta_{||}$ is argued to be small [7].

Meanwhile, it was proposed that the SPT state may lead to a gapless edge state even in the gapped bulk state, which, together with the bulk critical modes, leads to nonordinary SCBs in the appropriate edge [10]. This scenario is verified in coupled spin-1 Haldane chains. [16]

In this section, we study the surface critical behavior on this dangling chain edge for the easy-plane XXZ models where the symmetry of the model is down to $U(1)$, and, therefore, the bulk transition belongs to the 3D $O(2)$ universality class. Considering the puzzling situation that occurs in the $SU(2)$ models, we here study both the $S = 1/2$ and the $S = 1$ models.

A. $S = 1/2$ models

Let us start with the $S = 1/2$ models. Consider the limit $g \rightarrow \infty$ where the dangling-chain edge is decoupled from the bulk, the edge should be a gapless and quasi-long-range ordered TLL [20, 21, 38], where the vortex excitation is suppressed. If such gapless states continues to the bulk critical point, we expect nonordinary SCBs as those found in the $SU(2)$ models, which can be considered the special transition point of the surface transition induced by surface engineering [11]. As a result, the scaled surface correlation length ξ_1/L should converge to a constant, different from the ordinary SCBs, where ξ/L goes to zero [10].

To test whether such behavior occurs or not, we calculated the scaled surface correlation length ξ_1/L on the dangling-chain edge for system sizes up to $L = 256$ at the bulk critical points of $\Delta = 0.5$ and $\Delta = 0.9$, respectively. To our surprise, we found that ξ_1/L diverges slowly with the system size L , as shown in Fig. 3(a).

To understand this observation, we then calculated

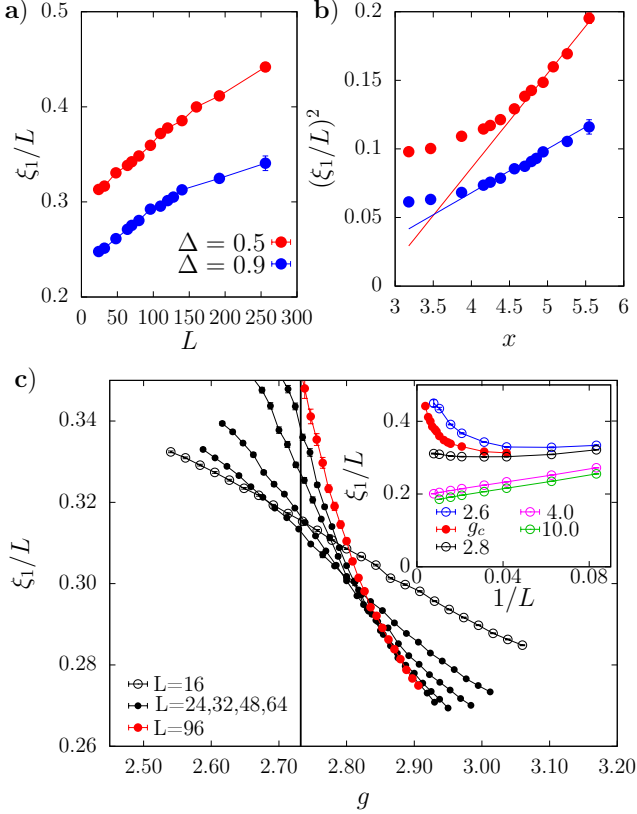


FIG. 3. a) The scaled surface correlation length ξ_1/L as a function of system size L for the $S = 1/2$ easy-plane CD models at bulk critical points g_c on a lin-lin scale. b) $(\xi_1/L)^2$ as a function of $x = \log(L/L_0)$ with L_0 constants different for $\Delta = 0.5$ and $\Delta = 0.9$. For large enough L , the curves become linear. c) The scaled surface correlation length ξ_1/L as a function of the bulk tuning parameter g for different system sizes for the $S = 1/2$ easy-plane CD model with $\Delta = 0.5$. The vertical line corresponds to the bulk critical point $g_c = 2.73227$. We see crossings near $g_{cs} \approx 2.85$. The inset plots ξ_1/L vs $1/L$ for different g .

ξ_1/L as a function of $g = J'/J$ away from the bulk critical point $g_c = 2.73227$ for the $S = 1/2$ $\Delta = 0.5$ CD easy-plane XXZ model. The results are plotted in Fig. 3(c). Remarkably, we see the curves of ξ_1/L vs. g for different system sizes cross roughly at $g_{cs} \approx 2.85$, larger than g_c .

One possible scenario is that a phase transition occurs on the dangling-chain edge to precede the bulk transition. This possibility is unusual at first sight: inside the gapped dimer phase, before the bulk critical point is approached, the coupling between the dangling-chain edge and the bulk can be considered weak. The Mermin-Wagner theorem [6] excludes the symmetry breaking phase in a (1+1)-D quantum system; therefore, no phase transition to an ordered phase is allowed when g is decreased. Instead, one expects that the $S = 1/2$ dangling-chain edge stays gapless or quasi-long-range ordered until the bulk critical point is reached, whereas critical fluctuations of the bulk

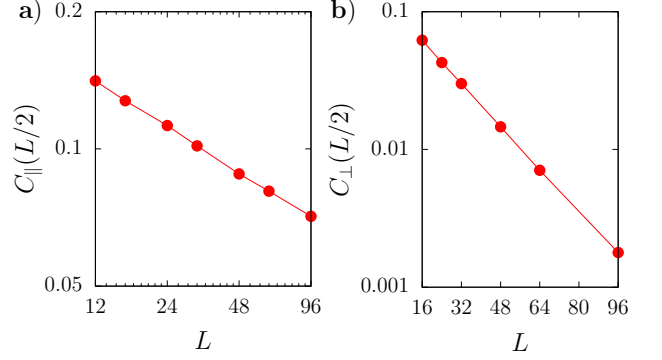


FIG. 4. Surface correlations on the dangling-chain edge for the $S = 1/2$ easy-plane CD model with $\Delta = 0.5$ at $g = 2.8$. a) $C_{\parallel}(L/2)$ vs L on a log-log scale. b) $C_{\perp}(L/2)$ vs L on a lin-log scale.

may induce effective long-range interactions along the chain, and a phase transition to an ordered state may occur. However, the Mermin-Wagner theorem does not exclude phase transition between two different short-range ordered phases [22, 23]. Thus, a transition in principle does not violate any physical law. In addition, as found in classical models, the changing of interaction range, not necessarily infinite, can drive the phase to another fixed point[24].

To better understand the results and further explore the physics properties of the surface state, we calculated the surface correlation function $C_{\parallel}(L/2)$ and $C_{\perp}(L/2)$, and the squared surface staggered magnetization m_{s1}^2 .

We first study the surface state at $g = 2.8$ between the bulk critical point $g_c = 2.73227$ and the surface transition point $g_{cs} \approx 2.85$, where the bulk is in a gapped disordered phase of the $S = 1/2$ CD XXZ model with $\Delta = 0.5$. We find that $C_{\perp}(L/2)$ shows an exponential decay, as illustrated in Fig. 4(b). Fitting $C_{\perp}(L)$ according to the following equation

$$C_{\perp}(L) = ae^{-L/\xi_{\perp}}, \quad (15)$$

we obtain $\xi_{\perp} = 22.4(2)$. It is evident that the bulk is gapped from the surface state at $g = 2.8$. As a result, we do not expect long-range order on the surface.

To confirm that there is no long-range order on the (1+1)-D dangling-chain edge, we fit $C_{\parallel}(L/2)$ according to the following scaling form:

$$C_{\parallel}(L/2) = C_{\parallel} + aL^{-(d+z-2+\eta_{\parallel})}, \quad (16)$$

where $C_{\parallel} \neq 0$ gives the long-range order parameter, and a is an unknown constant. The data of $C_{\parallel}(L/2)$ vs. L are plotted in Fig. 4(a) on a log-log scale. We find $C_{\parallel} = 0.013(7)$, and $\eta_{\parallel} = -0.62(3)$. The fit is good, but the magnitude of C_{\parallel} is within two times the error bar. We conclude that it is actually zero.

We then tried to fit $C_{\parallel}(L/2)$ according to Eq. (10). We find statistically sound fits for $L \geq 12$ without the

ω term and obtain $\eta_{\parallel} = -0.670(5)$. This fitting result is stable under further exclusion of small system sizes.

However, the power-law decay of the spin-spin correlation cannot support the divergence of ξ_1/L found in the region between g_c and g_{cs} , see Fig. 3(c). Inspired by the recently proposed extraordinary-log phase at the bulk critical point[7], we propose, in this phase, the correlation function $C_{\parallel}(L)$ decays as a power of $\log(L/L_0)$, i.e.,

$$C_{\parallel}(L) \propto \log(L/L_0)^{-q} \quad (17)$$

where q is an unknown exponent. At $g = 2.77$, slightly closer to g_c , we calculated C_{\parallel} and m_{s1}^2 up to $L = 192$. The results are shown in Fig. 5. We fit $C_{\parallel}(L/2)$ and $m_{s1}(L)$ according to Eq. (17). We find statistically sound fit with $L_{min} \geq 24$ for both quantities, as illustrated in Fig. 5(b). However, the fitting results are not stable as more system sizes are excluded. Instead, fitting $C_{\parallel}(L/2)$ according to Eq. (10) gives statistically sound results for $L_{min} \geq 16$, which are stable upon further excluding systems sizes. Similarly, fitting $m_{s1}^2(L)$ according to Eq. (12) offers good results for $L_{min} \geq 24$ and the fits are stable for further excluding small system sizes. The fits are shown in Fig. 5(a).

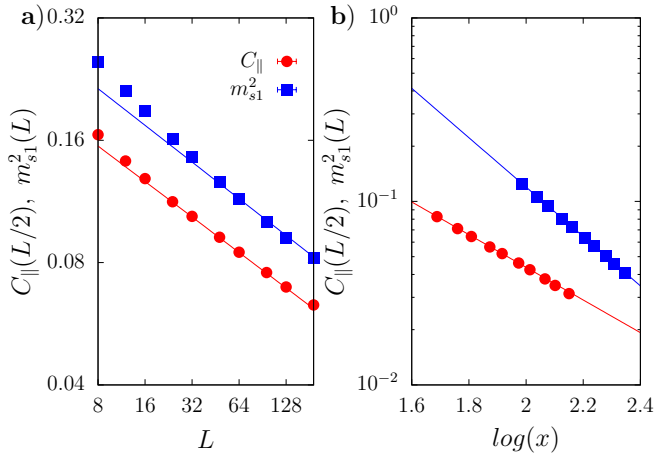


FIG. 5. The surface behaviors of the $S = 1/2$ easy-plane CD model with $\Delta = 0.5$ at $g = 2.77$. a) The surface squared antiferro-magnetization m_{s1}^2 and the surface correlation function $C_{\parallel}(L/2)$ vs $1/L$. b) $C_{\parallel}(L/2)$ and $m_{s1}^2(L)$ vs $x = \log(L/L_0)$ on a log-log scale with $L_0 = 0.036(15)$ for $C_{\parallel}(L/2)$ and $L_0 = 0.006(1)$ for $m_{s1}^2(L)$. The lines are fitting curves.

Although we cannot exclude the possibility that there exists a surface phase transition preceding the bulk transition, our data do not support this scenario. Since the crossing points are rather close to the bulk critical point where the bulk correlation length is large, we turn to believe that the divergence of ξ_1/L at $g > g_c$ are results of the bulk critical behavior. It is more likely that the correlation behaves finally cross over to normal TLL behavior.

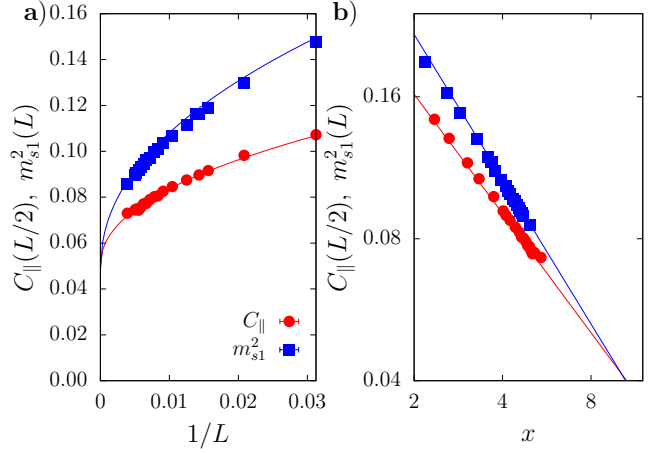


FIG. 6. The surface behaviors of the $S = 1/2$ easy-plane CD model with $\Delta = 0.5$ at the bulk critical point. a) The surface squared antiferro-magnetization m_{s1}^2 and the surface correlation function $C_{\parallel}(L/2)$ vs $1/L$. b) $C_{\parallel}(L/2)$ and $m_{s1}^2(L)$ vs $x = \log(L/L_0)$ on a log-log scale with $L_0 = 1.2(1)$ for $C_{\parallel}(L/2)$ and $L_0 = 1.8(7)$ for $m_{s1}^2(L)$. The lines are fitting curves.

We now move to the bulk critical point g_c .

In general, the scaling behavior in Eq. (16) is expected for extraordinary SCBs where the surface orders preceding the bulk when g is decreased, and exhibits extra singularities at the bulk critical point, for example, at the bulk critical point of a classical $O(n)$ model in dimensions $d > 3$ with large surface couplings. Furthermore, according to Eq. (6), we expect similar behavior of m_{s1}^2

$$m_{s1}^2(L) = m_{s1}^2 + bL^{2y_{h1}-2(d+z-1)} \quad (18)$$

with magnetization $m_{s1}^2 \approx C_{\parallel}$ and an unknown constant b . The results of $C_{\parallel}(L/2)$ and $m_{s1}^2(L)$ vs. $1/L$ at the bulk critical point g_c for the $S = 1/2$ CD easy-plane XXZ model with $\Delta = 0.5$ are shown in Fig. 6(a).

However, for a classical $O(2)$ model in three dimensions, the conclusion is controversial. At sufficiently large surface couplings, the surface should undergo a BKT transition to a quasi-long-ranged order before the bulk orders when the temperature is lowered down. When the bulk critical point is approached, Deng *et al.* proposed that the surface becomes long-range ordered due to long-range interactions induced by critical fluctuations; therefore, the order parameter has a jump[5]. As a result, the surface magnetization m_1^2 follows the scaling form Eq. (18) with $m_{s1}^2(L)$ replaced by $m_1^2(L)$. The nonzero m_1^2 and the exponent y_{h1} describing the power-law decay of the surface magnetization are found numerically[5]. However, Deng *et al.* offered another possibility that the surface magnetization still decays to zero in a power-law[5]. Moreover, a slightly different exponent y_{h1} was found by using the same data. For the reader's convenience, we list both results in Table III.

If the former scenario is realized on the dangling-chain surface in our QAF easy-plane model, we expect the sur-

face state to lie in an extraordinary state similar to that of the classical $O(n)$ model with dimension $d > 3$, which means $C_{\parallel}(L)$ behaves as Eq. (16) with $C_{\parallel} \neq 0$.

We tried to fit Eqs. (16) and (18) to our data. By gradually discarding small system sizes, we obtained a statistically sound fit without correction to scaling term. From correlation data $C_{\parallel}(L)$, we find asymptotic value $C_{\parallel} = 0.049(2)$ and $\eta_{\parallel} = -0.55(2)$, for $\Delta = 0.5$. For $\Delta = 0.9$, we estimated $C_{\parallel} = 0.033(2)$, and $\eta_{\parallel} = -0.41(2)$. By fitting the magnetization data, we find $m_{s1}^2 = 0.048(4)$ and $y_{h1} = 1.77(2)$ for $\Delta = 0.5$; $m_{s1}^2 = 0.034(2)$ and $y_{h1} = 1.69(1)$ for $\Delta = 0.9$. The fitting functions for $\Delta = 0.5$ are graphed in Fig. 6(a). The above results are listed in Table III. The estimated η_{\parallel} and y_{h1} for both Δ satisfy the scaling relation Eq. (14). The two constants C_{\parallel} and m_{s1}^2 are also in good agreement.

Though the values of C_{\parallel} and m_{s1}^2 found by our fitting are very small, their magnitudes are much larger than the corresponding error bars. It is also possible to fit without C_{\parallel} and m_{s1}^2 , but both fits to $C_{\parallel}(L/2)$ and $m_{s1}^2(L)$ give much worse fitting performance, even when the corrections to scaling are included. We therefore exclude this possibility.

We have also calculated the $C_{\perp}(L/2)$ at g_c . The correlation $C_{\perp}(L/2)$ of the extraordinary SCBs should scale as Eq. (11), but with a different η_{\perp} from that of the ordinary SCBs. By fitting according to Eq. (11), we find $\eta_{\perp} = -0.415(2)$ for $\Delta = 0.5$ and $\eta_{\perp} = -0.43(1)$ for $\Delta = 0.9$. These results are also listed in Table III. Indeed, they are different from η_{\perp} of the dangling-ladder edge.

Recently, Metlitski [7] proposed a theory based on RG arguments that an extraordinary-log phase may occur on the surface of the classical 3D $O(2)$ model when the surface couplings are strong enough. The quasi-long-range ordered surface phase undergoes a phase transition to the extraordinary-log phase, while stiffness of the surface order parameter diverges logarithmically. Such a transition is different from the suggestion proposed in [5] that a first-order transition with a jump of order parameter occurs when the bulk critical point approaches from the quasi-long-range ordered surface phase. The extraordinary-log state is a state less ordered than the long-range ordered state but more ordered than the quasi-long-range ordered state, in which the correlation function decays as a power of the logarithm of distance [7]. Numerical works on classical 3D $O(3)$ and 3D $O(2)$ models support the existence of such a phase [8, 9].

We then explored the possibility that the surface state at g_c is the extraordinary-log state. As proposed in [7], in such a state, the correlation function $C_{\parallel}(L/2)$ decays as a power of $\log(L/L_0)$, in the form of Eq. (17). Such behavior has been observed with $q = 0.59(2)$ on the surface of the critical 3D classical $O(2)$ model with sufficiently enhanced surface couplings [9]; see also Table III. We replot the surface parallel correlation function $C_{\parallel}(L/2)$ on the dangling-chain surface for the $S = 1/2$ CD easy-plan models in Fig. 6(b) on a log-log scale with

$x = \log(L/L_0)$. We observe a good straight curve. By gradually excluding small system sizes, we obtain statistically sound fits of the data according to Eq. (17). The best fits show $q = 0.82(2)$ and $L_0 = 1.2(1)$ for $\Delta = 0.5$, and $q = 1.03(2)$ and $L_0 = 1.26(9)$ for $\Delta = 0.9$ in the CD model. These results are listed in Table III. The fitting curve for the $\Delta = 0.5$ model is graphed in Fig. 6(b).

Furthermore, the extraordinary-log scaling offers another scenario to understand the divergence of ξ_1/L : according to the extraordinary-log scaling, the TLL parameter diverges logarithmically with the bulk correlation length as one approaches g_c [39], leading to the divergence of ξ_1/L near g_c .

The finite-size behavior Eq. (17) suggests that the surface magnetization $m_{s1}(L)$ also decays logarithmically with the same exponent q . We then tried to fit this formula to our $m_{s1}^2(L)$ data. However, the fits for both the $\Delta = 0.5$ and $\Delta = 0.9$ $S = 1/2$ models were not stable when we excluded small system sizes gradually. The asymptotic behaviors of $C_{\parallel}(L/2)$ and $m_{s1}^2(L)$ were also very different, as shown in Fig. 6(b) for $\Delta = 0.5$.

In addition, in recent work on the SCBs of an improved model in the classical 3D $O(3)$ universality class [8], where the extraordinary-log phase is verified at strong surface couplings, it is further proposed that ξ_1/L scales as

$$(\xi_1/L)^2 = \frac{\alpha}{\pi(n-1)} \log(L/L_0) \quad (19)$$

with α a constant for the $O(n)$ model and π represents the antiferromagnetic momentum. Here, we try to fit this ansatz to our ξ_1/L data. We again find statistically sound fits when small system sizes are excluded. The results are, as listed in Table III, $\alpha = 0.22(3)$, $L_0 = 16(8)$ for $\Delta = 0.5$ and $\alpha = 0.10(1)$, $L_0 = 7(3)$ for $\Delta = 0.9$, respectively. These results are demonstrated by replotting the rescaled surface correlation length $(\xi_1/L)^2$ as functions of $x = \log(L/L_0)$, with L_0 set to the fitting results, in Fig. 3(b). The curves are only linear for sufficiently large system sizes.

However, the values of α and q estimated here do not agree with the corresponding values of the classical $O(2)$ model found in [9], and they do not satisfy the scaling relation

$$q = \frac{n-1}{2\pi\alpha}, \quad (20)$$

predicted in [7], with n being the number of components of the classical spin.

Metlitski also proposed a possible state in the extraordinary-log fixed point with coexisting charge-density-wave order for the quantum $O(2)$ model. We have calculated the surface correlation $C_{\parallel}^Z(L/2)$ that averages $C^Z(i, j)$ between two surface spins i and j at the longest distance $L/2$ over the dangling chain. We find that the correlation goes to zero as $L \rightarrow \infty$. Thus, no charge-density-wave order is found.

TABLE III. Surface critical properties on the dangling-chain edge of the easy-plane CD models with $S = 1/2$ and $S = 1$. The SCBs of the classical 3D O(2) model at large surface coupling are also listed here for comparison. Here, η_{\parallel} are calculated using the scaling law $\eta_{\parallel} = 3 - 2y_{h1}$.

| Type | Δ | C_{\parallel} | $m_{s1}^2(m_1^2)$ | $y_{h1}^{(1)}$ | η_{\parallel} | η_{\perp} | q | α |
|--------------|----------|-----------------|-------------------|----------------|--------------------|----------------|------------|-------------|
| $S = 1/2$ | 0.5 | 0.049(2) | 0.048(4) | 1.77(2) | -0.55(2) | -0.415(2) | 0.82(2) | 0.22(3) |
| | 0.9 | 0.033(2) | 0.034(2) | 1.69(1) | -0.41(2) | -0.43(1) | 1.03(2) | 0.10(1) |
| $S = 1$ | 0.9 | 0.31(1) | 0.34(2) | 1.76(2) | -0.55(2) | -0.418(2) | 0.6(1) | 0.13(7) |
| Classical XY | 0 | — | 0.222[5] | 1.812(5) [5] | -0.62(1) | | 0.59(2)[9] | 0.27(2) [9] |
| | | | — | 1.9675(30)[5] | -0.935(6) | | | |

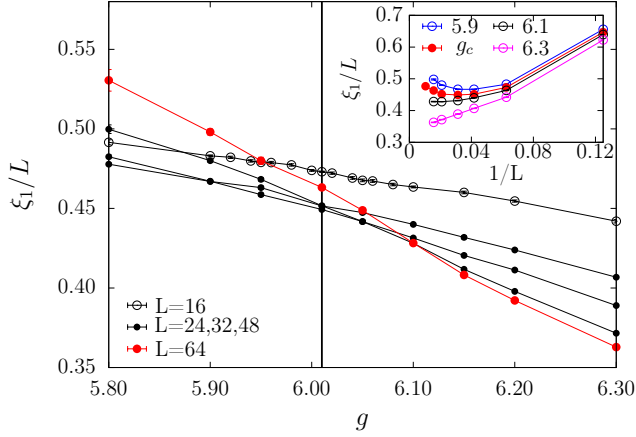


FIG. 7. The scaled surface correlation length ξ_1/L on the dangling-chain edge of the $S = 1$ easy-plane CD model with $\Delta = 0.9$ vs g for different system sizes L , showing a surface transition in the bulk gapped phase. The vertical line corresponds to the bulk critical point $g_c = 6.01$. The inset plots ξ_1/L vs $1/L$ for different g , showing divergence of ξ_1/L at g_c .

Considering all these analyses, for the $S = 1/2$ easy-plane XXZ model, we conclude that our numerical results support an extraordinary transition on the dangling-chain surface with a long-range order established by effective long-range interactions due to bulk critical fluctuations. Moreover this suggests the possibility that the state is an extraordinary-log state seems unlikely. The extraordinary-log scenario is also excluded for the SU(2) CD model.[40]

B. $S = 1$ model

To further investigate the nature of the dangling-chain surface, we also performed simulations for the $S = 1$ CD easy-plane model with $\Delta = 0.9$.

We find a surface transition in the bulk gapped phase, when g is adapted, by calculating the dimensionless ratio ξ_1/L as a function of g for different system sizes. As shown in Fig. 7, the curves of ξ_1/L show crossings that converge to a value around $g_{cs} \simeq 6.1$, larger than the bulk critical point $g_c = 6.01$ for the $S = 1$ CD easy-plane model with $\Delta = 0.9$, in the gapped bulk phase,

indicating a phase transition. Different from the $S = 1/2$ case, the edge is an $S = 1$ chain with a Haldane gap at the large g limit; therefore, this transition can be understood as a BKT transition in a (1+1)-D system. Without topological terms and thanks to the dangling settings, the system is analogous to the 3D classical O(2) model with strong surface couplings, which lead to the BKT transition in the bulk disordered phase when the temperature is lowered. Indeed, $C_{\parallel}(L/2)$ shows a power-law decay $1/r^x$ at $g = 6.1$. Fitting for L in the range from 16 to 64, we find $x = 0.22(2)$, which is close to $1/4$ at the BKT transition.

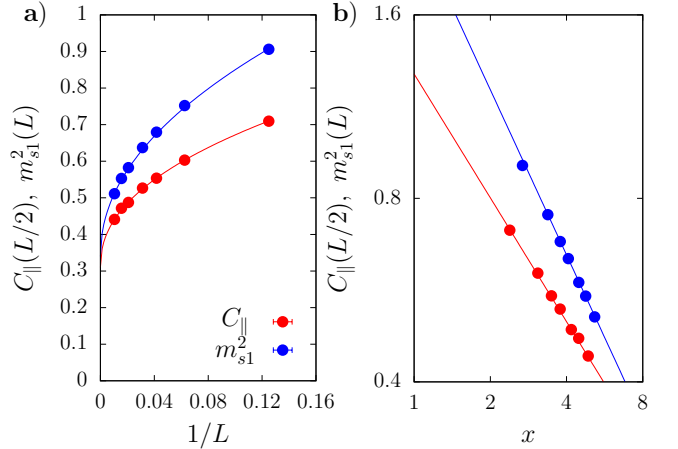


FIG. 8. The surface behaviors of the $S = 1$ easy-plane CD model with $\Delta = 0.9$ at the bulk critical point. a) The surface squared antiferro-magnetization m_{s1}^2 and the surface correlation function $C_{\parallel}(L/2)$ vs $1/L$. b) $C_{\parallel}(L/2)$ and $m_{s1}^2(L)$ vs $x = \log(L/L_0)$ on a log-log scale with $L_0 = 1.5(1.0)$ for $C_{\parallel}(L/2)$ and $L_0 = 0.5(4)$ for $m_{s1}^2(L)$. The lines are fitting curves.

We then studied the surface critical behavior at the bulk critical point $g_c = 6.01$. The results of $C_{\parallel}(L/2)$ and $m_{s1}^2(L)$ vs. $1/L$ at g_c are shown in Fig. 8(a). Since $g_c < g_{cs}$ and no topological terms available for the $S = 1$ chain and dangling settings, we expect a similar SCB to that in the classical 3D O(2) model with surface coupling enhanced. We therefore try to fit the results of $C_{\parallel}(L/2)$ using Eq. (16) and $m_{s1}^2(L)$ using Eq. (18) as expected for the extraordinary SCBs of the classical 3D O(2) model, where long-range order is induced by effective long-range

couplings due to critical modes, as proposed in [5].

From data of $C_{\parallel}(L/2)$, we find $C_{\parallel} = 0.31(2)$, and $\eta_{\parallel} = -0.55(2)$, for system sizes in the region $L \in [8, 64]$. The fit is statistically sound. By fitting Eq. (18) to $m_{s1}^2(L)$, we find $m_{s1}^2 = 0.34(2)$ and $y_{h1} = 1.76(2)$. These results are listed in Table III.

It is somewhat surprising that the values of C_{\parallel} and m_{s1}^2 are much larger than those of the $S = 1/2$ case. Semiclassically, the length of the $S = 1$ spin is $\sqrt{2}$, and the length of the $S = 1/2$ is $\sqrt{3}/2$. In this sense, if the models are in the same classical states, this value of C_{\parallel} (for $S = 1$) is too large and cannot be simply attributed to the size of the spin vector. This suggests that the quantum character of the $S = 1/2$ model is very important. However, the exponents η_{\parallel} and y_{h1} for the $S = 1$ model are close to those of the $S = 1/2$ SCB.

The behavior of $C_{\perp}(L/2)$ apparently follows the standard scaling behavior Eq. (11). From data of $C_{\perp}(L/2)$, we find statistically sound fit in the region $L \in [8, 64]$. The fitting results, listed in Table III, are $\eta_{\perp} = -0.418(2)$.

Considering recent progress in the SCBs of the 3D O(2) model [9], it is tempting to fit Eq. (17) to the $C_{\parallel}(L/2)$ data and fit Eq. (19) to the ξ_1/L data of the $S = 1$ model. We find a statistically sound fit with $q = 0.6(1)$ and $L_0 = 1.5(1.0)$ for Eq. (17). The data and fitting curves are plotted on a log-log scale in Fig. 8(b). The constants $\alpha = 0.13(7)$ and $L_0 = 0.3(6)$ in Eq. (19) were estimated. All the results are summarized in Table III. It is interesting that the exponent q equals the value of the classical model with $q = 0.59(2)$. However, the value of α is different from the corresponding value of the classical model, and the relation Eq. (20) is not satisfied. In addition, we have also fit $m_{s1}^2(L)$ data with Eq. (17) and found statistical sound fit $q = 0.9(2)$ and $L_0 = 0.5(4)$, as shown in Fig. 8.

While we cannot exclude the scenario in which the SCB of the dangling chain edge of the $S = 1$ CD model belongs to the extraordinary fixed point for normal O(n) model, especially when considering the large nonzero values of C_{\parallel} and m_{s1}^2 , however, from the point of quantum and classical mapping, it is likely that the SCBs are of the new extraordinary-log type.

V. CONCLUSION

Using unbiased quantum Monte Carlo simulations, we have studied the 2D columnar dimerized quantum anti-ferromagnetic XXZ model with easy-plane anisotropy for both $S = 1/2$ and $S = 1$ spins. We have paid particular attention to the surface behaviors on two different surfaces exposed by cutting a row of strong bonds or cutting a row of weak bonds along the direction perpendicular to the strong bonds of a periodic system.

We found ordinary SCBs on the dangling-ladder sur-

face for both $S = 1/2$ and $S = 1$ systems, but completely different surface behaviors on the dangling-chain surface for the $S = 1/2$ and $S = 1$ models.

On the dangling-chain surface, the $S = 1$ model behaves akin to the classical 3D XY model with large surface couplings. We find a BKT transition in the bulk gapped phase, and the surface seems to show extraordinary-log behaviors at the bulk critical point.

For the $S = 1/2$ model, we find unexpected crossings of scaled surface correlation length ξ_1/L in the bulk gapped phase, considering the surface is already critical as a TLL at the large g limit. One scenario to explain this is that there is a new surface state, between the transition point and the bulk critical point, with spin-spin correlation $C_{\parallel}(L/2)$ decaying as a power of $\log(L)$. As a result, ξ_1/L diverges in this phase, as well as at the bulk critical point. However, fitting of numerical data upto $L = 192$ does not support this scenario, the fits are not stable upon gradually excluding small system sizes. The correlation behaves seem cross over to normal TLL power law behavior, as small system sizes are excluded in the fits. In the end, it is more plausible that the divergence of ξ_1/L are results of bulk critical behavior.

At the bulk critical point, our numerical results support an extraordinary SCB with a long-range order established by effective long-range interactions due to bulk critical correlations. The possibility that the surface shows extraordinary-log behavior seems unlikely. This is very different from the SU(2) dimerized Heisenberg model, where the surface transition at the dangling-chain edge is found to be nonordinary, but also not extraordinary[11, 12], in the sense that C_{\parallel} and m_{s1}^2 were found to converge to zero.

It would be very interesting to further investigate the phase transition from TLL to the critical state in the bulk gapped phase.

ACKNOWLEDGMENTS

We thank Max Metlitski for pointing out the correct form of Eq. (19). W.Z. and W.G. were supported by the National Natural Science Foundation of China under Grant No. 11775021 and No. 11734002. C.D. was supported by the National Natural Science Foundation of China under Grant No. 11975024, No. 11774002 and No. 62175001 and the Anhui Provincial Supporting Program for Excellent Young Talents in Colleges and Universities under Grant No. gxyqZD2019023. L.Z. was supported by the National Natural Science Foundation of China under Grant No. 11804337 and No. 12174387, the Strategic Priority Research Program of CAS under Grant No. XDB28000000 and the CAS Youth Innovation Promotion Association. The authors acknowledge support extended by the Super Computing Center of Beijing Normal University.

-
- [1] K. Binder, [Phase Transitions and Critical Phenomena](#), edited by C. Domb and J. L. Lebowitz, Vol. 8 (Academic Press, London, 1983) pp. 2–134.
- [2] K. Binder and P. C. Hohenberg, Surface effects on magnetic phase transitions, [Phys. Rev. B](#) **9**, 2194 (1974).
- [3] H. W. Diehl, [Phase Transitions and Critical Phenomena](#), edited by C. Domb and J. L. Lebowitz, Vol. 10 (Academic, London, 1986) pp. 75–267.
- [4] H. W. Diehl, The theory of boundary critical phenomena, [International Journal of Modern Physics B](#) **11**, 3503 (1997).
- [5] Y. Deng, H. W. J. Blöte, and M. P. Nightingale, Surface and bulk transitions in three-dimensional $O(n)$ models, [Phys. Rev. E](#) **72**, 016128 (2005).
- [6] N. D. Mermin and H. Wagner, Absence of ferromagnetism or antiferromagnetism in one- or two-dimensional isotropic heisenberg models, [Phys. Rev. Lett.](#) **17**, 1133 (1966).
- [7] M. A. Metlitski, Boundary criticality of the $o(n)$ model in $d=3$ critically revisited, arXiv preprint arXiv:2009.05119 (2020).
- [8] F. Parisen Toldin, Boundary critical behavior of the three-dimensional heisenberg universality class, [Phys. Rev. Lett.](#) **126**, 135701 (2021).
- [9] M. Hu, Y. Deng, and J.-P. Lv, Extraordinary-log surface phase transition in the three-dimensional xy model (2021), [arXiv:2104.05152 \[cond-mat.stat-mech\]](#).
- [10] L. Zhang and F. Wang, Unconventional surface critical behavior induced by a quantum phase transition from the two-dimensional affleck-kennedy-lieb-tasaki phase to a néel-ordered phase, [Phys. Rev. Lett.](#) **118**, 087201 (2017).
- [11] C. Ding, L. Zhang, and W. Guo, Engineering surface critical behavior of $(2+1)$ -dimensional $o(3)$ quantum critical points, [Phys. Rev. Lett.](#) **120**, 235701 (2018).
- [12] L. Weber, F. Parisen Toldin, and S. Wessel, Nonordinary edge criticality of two-dimensional quantum critical magnets, [Phys. Rev. B](#) **98**, 140403 (2018).
- [13] L. Weber and S. Wessel, Nonordinary criticality at the edges of planar spin-1 heisenberg antiferromagnets, [Phys. Rev. B](#) **100**, 054437 (2019).
- [14] Z.-C. Gu and X.-G. Wen, Tensor-entanglement-filtering renormalization approach and symmetry-protected topological order, [Phys. Rev. B](#) **80**, 155131 (2009).
- [15] F. Pollmann, A. M. Turner, E. Berg, and M. Oshikawa, Entanglement spectrum of a topological phase in one dimension, [Phys. Rev. B](#) **81**, 064439 (2010).
- [16] W. Zhu, C. Ding, L. Zhang, and W. Guo, Surface critical behavior of coupled haldane chains, [Phys. Rev. B](#) **103**, 024412 (2021).
- [17] V. L. Berezinsky, Destruction of long range order in one-dimensional and two-dimensional systems having a continuous symmetry group. I. Classical systems, [Sov. Phys. JETP](#) **32**, 493 (1971).
- [18] V. L. Berezinsky, Destruction of Long-range Order in One-dimensional and Two-dimensional Systems Possessing a Continuous Symmetry Group. II. Quantum Systems., [Sov. Phys. JETP](#) **34**, 610 (1972).
- [19] J. M. Kosterlitz and D. J. Thouless, Ordering, metastability and phase transitions in two-dimensional systems, [Journal of Physics C: Solid State Physics](#) **6**, 1181 (1973).
- [20] S.-i. Tomonaga, Remarks on Bloch’s Method of Sound Waves applied to Many-Fermion Problems, [Progress of Theoretical Physics](#) **5**, 544 (1950), <https://academic.oup.com/ptp/article-pdf/5/4/544/5430161/5-4-544.pdf>.
- [21] J. M. Luttinger, An exactly soluble model of a many-fermion system, [Journal of Mathematical Physics](#) **4**, 1154 (1963), <https://doi.org/10.1063/1.1704046>.
- [22] E. Domany, M. Schick, and R. H. Swendsen, First-order transition in an xy model with nearest-neighbor interactions, [Phys. Rev. Lett.](#) **52**, 1535 (1984).
- [23] H. W. J. Blöte, W. Guo, and H. J. Hilhorst, Phase transition in a two-dimensional heisenberg model, [Phys. Rev. Lett.](#) **88**, 047203 (2002).
- [24] X. Qian, Y. Deng, Y. Liu, W. Guo, and H. W. J. Blöte, Equivalent-neighbor potts models in two dimensions, [Phys. Rev. E](#) **94**, 052103 (2016).
- [25] A. W. Sandvik, Computational studies of quantum spin systems, [AIP Conference Proceedings](#) **1297**, 135 (2010).
- [26] O. F. Syljuåsen and A. W. Sandvik, Quantum monte carlo with directed loops, [Phys. Rev. E](#) **66**, 046701 (2002).
- [27] A. W. Sandvik, Stochastic series expansion method with operator-loop update, [Phys. Rev. B](#) **59**, R14157 (1999).
- [28] N. Ma, P. Weinberg, H. Shao, W. Guo, D.-X. Yao, and A. W. Sandvik, Anomalous quantum-critical scaling corrections in two-dimensional antiferromagnets, [Phys. Rev. Lett.](#) **121**, 117202 (2018).
- [29] H. G. Evertz, The loop algorithm, [Advances in Physics](#) **52**, 1 (2003), <https://doi.org/10.1080/0001873021000049195>.
- [30] A. Dorneich and M. Troyer, Accessing the dynamics of large many-particle systems using the stochastic series expansion, [Phys. Rev. E](#) **64**, 066701 (2001).
- [31] M. Matsumoto, C. Yasuda, S. Todo, and H. Takayama, Ground-state phase diagram of quantum heisenberg antiferromagnets on the anisotropic dimerized square lattice, [Phys. Rev. B](#) **65**, 014407 (2001).
- [32] M. P. Nightingale and H. W. J. Blöte, Universality of surface correlation functions in three-dimensional models, [Phys. Rev. B](#) **48**, 13678 (1993).
- [33] D. P. Landau, R. Pandey, and K. Binder, Monte carlo study of surface critical behavior in the XY model, [Phys. Rev. B](#) **39**, 12302 (1989).
- [34] M. Barber, [Phase Transitions and Critical Phenomena](#), edited by C. Domb and J. L. Lebowitz, Vol. 8 (Academic Press, London, 1983) pp. 146–257.
- [35] T. C. Lubensky and M. H. Rubin, Critical phenomena in semi-infinite systems. i. ϵ expansion for positive extrapolation length, [Phys. Rev. B](#) **11**, 4533 (1975).
- [36] M. Campostrini, M. Hasenbusch, A. Pelissetto, P. Rossi, and E. Vicari, Critical behavior of the three-dimensional XY universality class, [Phys. Rev. B](#) **63**, 214503 (2001).
- [37] C.-M. Jian, Y. Xu, X.-C. Wu, and C. Xu, Continuous Néel-VBS Quantum Phase Transition in Non-Local one-dimensional systems with $SO(3)$ Symmetry, [SciPost Phys.](#) **10**, 33 (2021).
- [38] T. Giamarchi and O. U. Press, [Quantum Physics in One Dimension](#), International Series of Monographs on Physics (Clarendon Press, 2004).
- [39] M. A. Metlitski, (private communication).

- [40] C. Ding, W. Zhu, W. Guo, and L. Zhang, Special transition and extraordinary phase on the surface of a (2+1)-dimensional quantum heisenberg antiferromagnet (2021), [arXiv:2110.04762 \[cond-mat.str-el\]](#).

Appendix A: Bulk Critical Points

We determine the bulk quantum critical points of the two-dimensional columnar dimerized quantum antiferromagnetic easy-plane XXZ models with anisotropic parameter $\Delta < 1$ using finite-size scaling analyses, based on the SSE QMC simulations of the models on $L \times L$ square lattices with periodic boundary conditions. We set the inverse temperature β to $2L$ to obtain the properties of the zero-temperature quantum phase transition at the limit $L \rightarrow \infty$.

We measure the spin stiffness ρ_s^α along the α direction which is related to the winding number fluctuations as follows:

$$\rho_s^\alpha = \frac{1}{\beta} \langle W_\alpha^2 \rangle, \quad (\text{A1})$$

where $\alpha = x, y$, and $W_x(W_y)$ is the winding number in the x (y) direction, which is defined as

$$W_\alpha = (N_\alpha^+ - N_\alpha^-)/L \quad (\text{A2})$$

where N_α^+ (N_α^-) denotes the number of operators transporting spin in the positive (negative) α direction.

We take the following scaling ansatz, namely, the scaled spinstiffness $L\rho_s^\alpha$ is dimensionless to extrapolate quantum critical point g_c and the correlation length exponent ν

$$L\rho_s^\alpha(g, L) = f((g - g_c)L^{1/\nu}, L^{-\omega}), \quad (\text{A3})$$

where ν is the exponent for correlation length and ω is the leading exponent for the corrections to scaling. This is done by expanding the above equation to the second order of $(g - g_c)L^{1/\nu}$

$$\begin{aligned} L\rho_s^\alpha(g, L) = & c + a_1(g - g_c)L^{1/\nu} + a_2L^{-\omega_1} \\ & + b_1(g - g_c)^2L^{2/\nu} \\ & + b_2(g - g_c)L^{1/\nu - \omega_1} + b_3L^{-2\omega_1} \end{aligned} \quad (\text{A4})$$

then fitting the above formula to the data obtained from simulations.

Figure 9 shows the scaled spin stiffness $\rho_s^x L$, $\rho_s^y L$ and $\rho_s L$ as a function of g for various system sizes. We have done the fits for $\rho_s^x L$, $\rho_s^y L$ and $\rho_s L = \frac{1}{2}(\rho_s^x + \rho_s^y)L$. By gradually excluding data of small system sizes, we obtain statistically sound and stable fits of Eq. (A4) for $S = 1/2$ models with $\Delta = 0.5$ and $\Delta = 0.9$, and $S = 1$ model with $\Delta = 0.9$. The final estimates of g_c and ν are listed in Table I.

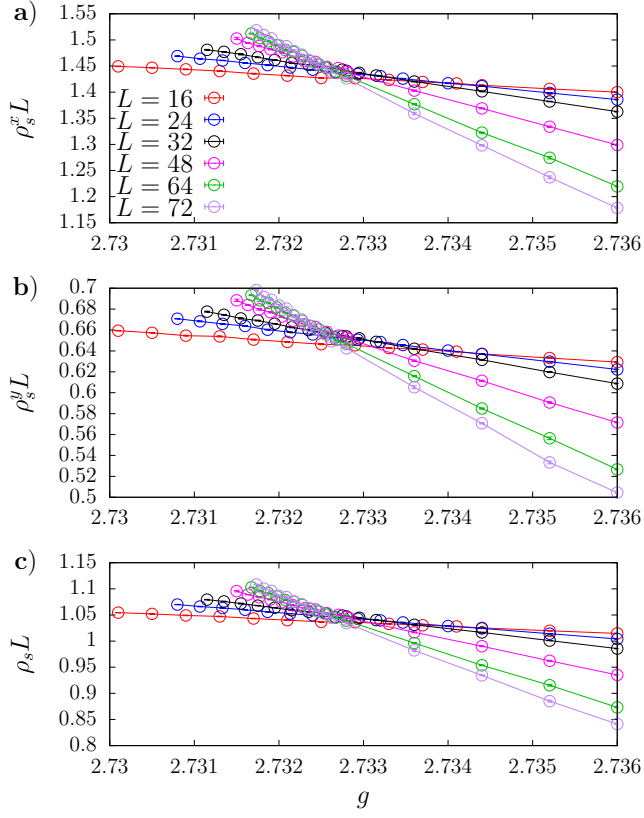


FIG. 9. The scaled spin stiffness of the $S = 1/2$ columnar dimerized XXZ model with $\Delta = 0.5$ for different system sizes L as a function of g . a) $\rho_s^x L$ vs g , b) $\rho_s^y L$ vs g , c) $\rho_s L$ vs g .